Fabrication of micro-axicons using direct-laser writing

Huang, He; Chen, Shijie; Zou, Hongmei; Li, Qing; Fu, Jian; Lin, Feng; Wu, X.

2014

Huang, H., Chen, S., Zou, H., Li, Q., Fu, J., Lin, F., et al. (2014). Fabrication of micro-axicons using direct-laser writing. Optics Express, 22(9), 11035-11042.

https://hdl.handle.net/10356/96659

https://doi.org/10.1364/OE.22.011035

Fabrication of micro-axicons using direct-laser writing

He Huang,[1] Shijie Chen,[1] Hongmei Zou,[1] Qing Li,[1] Jian Fu,[1] Feng Lin,[2] and X. Wu[1,*]

[1]*State Key Laboratory of Modern Optical Instrumentation, Department of Optical Engineering, Zhejiang University, Hangzhou, Zhejiang 310027, China*

[2]*School of Computer Engineering, Nanyang Technological University, 637553, Singapore*

xingkunwu@zju.edu.cn

Abstract: A novel direct-laser writing fabrication process for micro-axicons is demonstrated. A fiber-axicon-generated Bessel beam was utilized to write on UV-curable optical epoxy to form new axicons and axicon arrays, and geometrical parameters of the replicated epoxy axicons were analyzed in terms of both apex angle and proximity of the writing axicons. The shape of the fabricated axicons was demonstrated to be controllable through laser exposure, proximity, and apex angle of the source axicon, and the fabricated axicons are capable of generating a quality Bessel beam with an excellent focusing performance.

OCIS codes: (220.4000) Microstructure fabrication; (220.4610) Optical fabrication.

References and links

1. V. Garcés-Chávez, D. McGloin, H. Melville, W. Sibbett, and K. Dholakia, "Simultaneous micromanipulation in multiple planes using a self-reconstructing light beam," Nature **419**(6903), 145–147 (2002).
2. R. Arimoto, C. Saloma, T. Tanaka, and S. Kawata, "Imaging properties of axicon in a scanning optical system," Appl. Opt. **31**(31), 6653–6657 (1992).
3. A. Marcinkevicius, S. Juodkazis, S. Matsuo, V. Mizeikis, and H. Misawa, "Application of Bessel beams for microfabrication of dielectrics by femtosecond laser," Jpn. J. Appl. Phys. **40**(11A), 1197–1199 (2001).
4. M. Erdélyi, Z. L. Horvath, G. Szabo, Zs. Bor, F. K. Tittel, J. R. Cavallaro, and M. C. Smayling, "Generation of diffraction-free beams for application in optical microlithography," J. Vac. Sci. Technol. B **15**(2), 287–292 (1997).
5. R. Grunwald, U. Neumann, A. Rosenfeld, J. Li, and P. R. Herman, "Scalable multichannel micromachining with pseudo-nondiffracting vacuum ultraviolet beam arrays generated by thin-film axicons," Opt. Lett. **31**(11), 1666–1668 (2006).
6. V. Kebbel, U. Neumann, U. Griebner, and M. Piché, "Ultrafast spatiotemporal processing with thin-film micro-optics," Opt. Eng. **43**(11), 2518–2524 (2004).
7. J. Durnin, "Exact solutions for nondiffracting beams. I. The scalar theory," J. Opt. Soc. Am. A **4**(4), 651–654 (1987).
8. J. Durnin, J. J. Miceli, Jr., and J. H. Eberly, "Diffraction-free beams," Phys. Rev. Lett. **58**(15), 1499–1501 (1987).
9. J. M. Ward, D. G. O'Shea, B. J. Shortt, M. J. Morrissey, K. Deasy, and S. G. Nic Chormaic, "Heat-and-pull rig for fiber taper fabrication," Rev. Sci. Instrum. **77**(8), 083105 (2006).
10. S. K. Mohanty and K. S. Mohanty, "Single fiber optical tweezers for manipulation of microscopic objects," Proc. SPIE **6441**, 644116 (2007).
11. S. Cabrini, C. Liberale, D. Cojoc, A. Carpentiero, M. Prasciolu, S. Mora, V. Degiorgio, F. De Angelis, and E. Di Fabrizio, "Axicon lens on optical fiber forming optical tweezers, made by focused ion beam milling," Microelectron. Eng. **83**(4–9), 804–807 (2006).
12. C. Liberale, G. Cojoc, P. Candeloro, G. Das, F. Gentile, F. De Angelis, and E. Di Fabrizio, "Micro-optics fabrication on top of optical fibers using two-photon lithography," IEEE Photon. Technol. Lett. **22**(7), 474–476 (2010).
13. R. Grunwald, H. Mischke, and W. Rehak, "Microlens formation by thin-film deposition with mesh-shaped masks," Appl. Opt. **38**(19), 4117–4124 (1999).
14. J.-F. Fortin, G. Rousseau, N. McCarthy, and M. Piché, "Generation of quasi- Bessel beams and femtosecond optical X- waves with conical mirrors," Proc. SPIE **4833**, 876–884 (2003).
15. A. Žukauskas, M. Malinauskas, C. Reinhardt, B. N. Chichkov, and R. Gadonas, "Closely packed hexagonal conical microlens array fabricated by direct laser photopolymerization," Appl. Opt. **51**(21), 4995–5003 (2012).
16. S. Grilli, S. Coppola, V. Vespini, F. Merola, A. Finizio, and P. Ferraro, "3D lithography by rapid curing of the liquid instabilities at nanoscale," Proc. Natl. Acad. Sci. U.S.A. **108**(37), 15106–15111 (2011).
17. Y. L. Zhang, Q. D. Chen, H. Xia, and H. B. Sun, "Designable 3D nanofabrication by femtosecond laser direct writing," Nano Today **5**(5), 435–448 (2010).

#203763 - $15.00 USD Received 3 Jan 2014; revised 21 Mar 2014; accepted 22 Apr 2014; published 1 May 2014

18. T. Cizmár, "Optical traps generated by non-traditional beams," Ph.D. thesis, Masaryk University in Brno (2006).
19. J. M. Shaw, J. D. Gelorme, N. C. LaBianca, W. E. Conley, and S. J. Holmes, "Negative photoresists for optical lithography," IBM J. Res. Develop. **41**(1.2), 81–94 (1997).

1. Introduction

Currently micro-axicons are regarded as one of most important optical elements in micro-optics for their applications in various domains, including in optical tweezers [1], imaging [2], micro-fabrication [3] and lithography [4]. The integration of micro-axicons at the extremity of optical fibers offers the possibility of producing Bessel-like beams within a compact system well-suited for manipulating small particles such as biological cells. Micro-axicon arrays are also promising components for multichannel micromachining [5] and array beam generation at ultra-short pulse durations with broad spectral bandwidths [6].

Since its advent, several micro-axicon fabrication techniques have been previously devised [7, 8]. The mechanical heat-and-pull rig for fiber taper fabrication is simple and reproducible [9], but the apex angles of the generated axicons are relatively small, causing a negative effect on the generated Bessel beams. Chemical etching is a reproducible process that can provide axially symmetric conical lenses aligned to the fiber core [10], realizing various apex-angle axicons using glass corrosion chemicals such as hydroñuoric acid. Focused ion beam (FIB) technology can fabricate ideal axicons that produce well-defined Bessel-like beams, but fabrication speed and required equipment make this technique cost-ineffective [11]. Two-photon lithography can also be used to fabricate Axicons on the fiber end-face, quickly creating generic three-dimensional shapes using a single setup [12]. Micro-axicon arrays have also been produced by means of mask-shadowing in a vapor deposition procedure with masks fixed at certain distances to the substrates [13] or rotating relative to substrates [14]. This is a simple and cost-effective method to fabricate flat and smooth components, but their reproducibility and homogeneity for axicon fabrication depends on the vaporizing materials and other factors. Other techniques including direct laser photo-polymerization [15] and its combination with the application of electro-hydrodynamic pressure are also interesting approaches to fabricate axicons and arrays thereof [16].

In search of a promising fabrication process, much effort has been devoted to features including the ability to be continually printable on a substrate and cost-effective creation of highly consistent optical-quality 3D surfaces. We demonstrate in this study a novel fabrication process for both micro-axicons and axicon arrays by one-step laser direct writing. Instead of using the forming process of ultra-fast laser pulse scanning [17], a single laser pulse with a cone-shaped beam has been used to expose UV optical epoxy, producing axicons of various apex angles with an optical surface finishing and size uniformity. The use of selective laser exposure and epoxy re-flow forming process sets a less demanding fab-environment condition for low-loss optical component manufacture, compared to the mask photolithography techniques. Through controlling the writing parameters including beam shape, exposure, and development process, we were able to generate micro-axicons and arrays at various cone parameters with excellent optical quality.

2. Fabrication

The setup for laser direct-writing fabrication of axicons is illustrated in Fig. 1 (Upper), which includes following devices: an individual fiber-axicon (as shown in Fig. 2(b), custom made fiber-axicon on a G.652 fiber tip with an apex angle ranging from 75° to 125°, and a surface roughness of about 0.02 to 0.04μm) produced by mechanical polishing used to generate Bessel beams; a high precision (100 nm step-size) two-dimensional translation stage (moving directions indicated as X, Y) of high moving accuracy controlled by a PCI board C-843, both commercially available from PI (Physik Instrumente, Germany); a Z-axis translation stage used for vertical movement control of the fiber-axicon; and a light emitting diode (LED) providing illumination needed for in situ CMOS-monitoring of the fabrication sequence. The microscope camera measures the distance between tip of the fiber axicon and upper surface of UV curable epoxy (DSM, G.652 optical fiber secondary coating). The entire process of

#203763 - $15.00 USD Received 3 Jan 2014; revised 21 Mar 2014; accepted 22 Apr 2014; published 1 May 2014

direct-writing is automated by custom in-house programming environment. A laser diode (Sony, SLD3237VF) with a central wavelength of 405 nm was used for exposure.

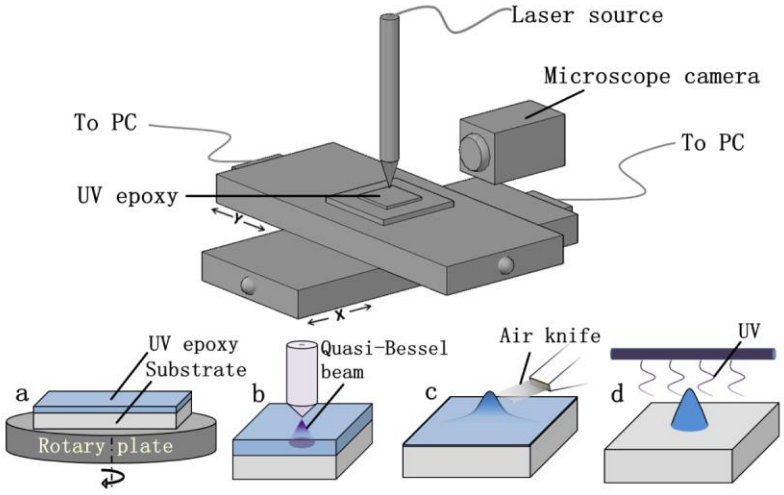

Fig. 1. (Upper) Schematic of setup for axicon fabrication; (Lower) a. Spin-coating of UV curable epoxy; b. Laser exposure with a Quasi-Bessel beam; c. Removing residual epoxy using an air knife; d. Post-exposure UV curing.

Figure 1(Lower) a-d displays the sequence of fabrication. UV curable optical epoxy was spin-coated onto a cover glass, and mounted on a sample holder for laser writing. The viscosity of the epoxy was kept at ~4800mPa·s@50s^{-1} to maintain a uniform coating thickness by controlling the working temperature at 20°C. The exposed viscous liquid pre-polymer then undergoes a cross-linking reaction upon UV exposure, and solidifies immediately. The unexposed pre-polymer was removed both mechanically and chemically.

For the exposed polymer, a post-exposure treatment was then conducted to develop direct-writing patterns. Instead of using traditional wet developing methods that were found to be difficult in maintaining fine feature of preliminarily solidified epoxy, we developed an air-knife-based method. Compressed air (0.2 Mpsi) was pressured out from air knife openings onto the substrate with variable angles ranging from 20° to 40° with respect to the substrate surface, driving the uncured epoxy off the substrate. The air knife was found to be capable of blowing off approximately 90% of the unexposed epoxy, while the remaining unexposed UV epoxy was cleaned off by spraying a small amount of ethanol onto the substrate to enhance the air knife developing process and to clean up any remaining residuals created during the knife-edge development. After this pattern developing process, the sample was placed into a UV irradiance chamber (a 20 W mercury lamp) for 4 minute, where the epoxy structure is thoroughly cured to reach a stable refractive index of 1.475. This developing process also improves surface finishing by re-flow of uncured epoxy over the cured structure, forming a smooth optical surface by the surface tension of UV epoxy. An optically satisfactory finish with a surface roughness below 0.05μm was obtained using the above methodology.

The setup is capable of generating various axicons depending on the laser beam profile and size of the UV illumination on the epoxy. With the fiber-axicon used in the experiment, a single mode laser beam traveling in the fiber was converted from a Gaussian profile to a Bessel-like beam (λ = 405 nm, minimum FWHM = 1.5 μm, maximum output power 20 mW). Being exposed to this Bessel-like beam, the UV epoxy was quickly cured and generated a shape based on the illumination beam profile, as shown in Fig. 2(a)-2(c). As shown in Fig. 2 (c), the basis and extended tip of the axicon can be distinguished, and in the following analysis only optical property of the extended tip is concerned.

#203763 - $15.00 USD Received 3 Jan 2014; revised 21 Mar 2014; accepted 22 Apr 2014; published 1 May 2014

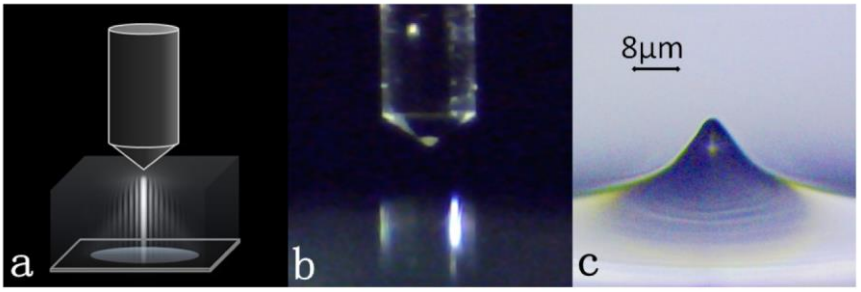

Fig. 2. (a) Schematic of the fabrication close-up, (b) Microscopic picture of fiber axicon above epoxy layer in primary curing step, (c) Microscopic image of the axicon fabricated by laser direct writing.

The intensity distribution of the quasi-Bessel beam from the axicon illuminated by a Gaussian beam can be calculated as follows [18]:

$$I(\rho,z)=\frac{I_0\pi k\sin(\alpha_0)}{2}\left[(F_1+F_2)^2J_0{}^2(k\rho\sin(\alpha_0))+(F_1-F_2)^2J_1{}^2(k\rho\sin(\alpha_0))\right] \quad (1)$$

$$F_1=\sqrt{z\tan\alpha_0+\rho}\cdot e^{-\left[\frac{z\tan\alpha_0+\rho}{w}\right]^2},\quad F_2=H(z\tan\alpha_0-\rho)\cdot\sqrt{z\tan\alpha_0-\rho}\cdot e^{-\left[\frac{z\tan\alpha_0+\rho}{w}\right]^2} \quad (2)$$

where ρ is the radial distance in cylindrical coordinates, w the half-width of the Gaussian beam waist, k the wave vector length, H(ztan(α_0)-ρ) a step function and α_0 the angle with which a vector normal to the conical surface of wavefront is coplanar with z axis; wherein $\alpha_0\cong(n_a\text{-}n_s)(\pi\text{-}\tau)/2n_s$ with na being refractive index of the axicon, ns the refractive index of the surrounding medium (air), and τ the apex angle of the axicon.

Equation (1) derives a spatial profile of the quasi-Bessel beam coming from the fiber axicon, as illustrated in Fig. 2(a). The focused beam is cone-shaped with multiple rings. A dotted curve in Fig. 3 shows an apex angle of the focused beam as a function of the apex angle of the fiber-axicon. From Eq. (1) it can also be derived that the center lobe intensity of beam will spread over to high order rings as the apex angle decreases, and its full width at half maximum (FWHM) of the center lobe will decrease. As a result, the apex angle of fabricated axicon decreases with increasing apex angle of fiber axicons used for Bessel beam generation in laser direct writing, while a fiber axicon with a small apex angle is expected to produce an epoxy axicon with a great angle and extended base. This trend was verified experimentally by employing axicons with difference apex angles, as shown in Fig. 3. Discrepancy between theoretical prediction and experimental measurement is mainly due to the fact that solidified volume includes two parts of fabricated axicon, basis and extended tip.

#203763 - $15.00 USD Received 3 Jan 2014; revised 21 Mar 2014; accepted 22 Apr 2014; published 1 May 2014

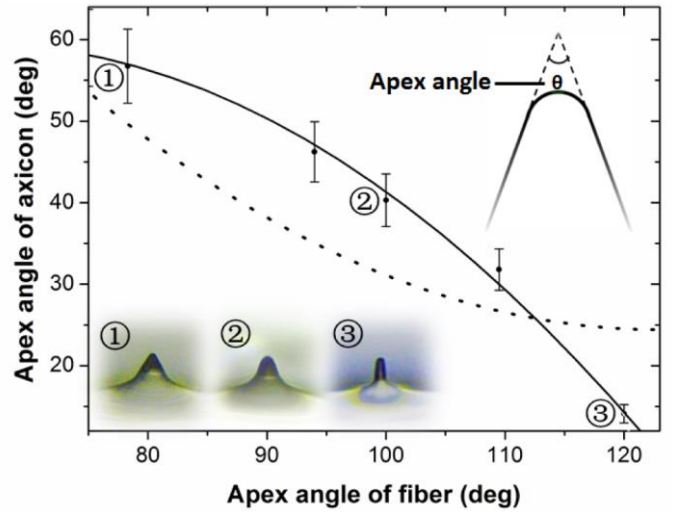

Fig. 3. Apex angle of the fabricated axicon as a function of apex angle of fiber axicon, with calculated result shown in dotted line; inserts (1)-(3) display microscopic images of fabricated axicons by using different fiber cone lenses.

When the apex angle of the fiber is small, the high order rings in the focused beam carry a high proportion of the power, and the central beam plays a minor role in the fabrication process. With the diffusion of photo-sensitizers activated by the laser, the apex angle of the axicon fabricated is bigger than the focused beam. The opposite situation is observed in the case of a large apex angle of the fiber cone, when the power carried in the high order rings in the focused beam are less important and the central lobe dominates. Consequently, the fabricated apex angle becomes smaller than that of the laser beam.

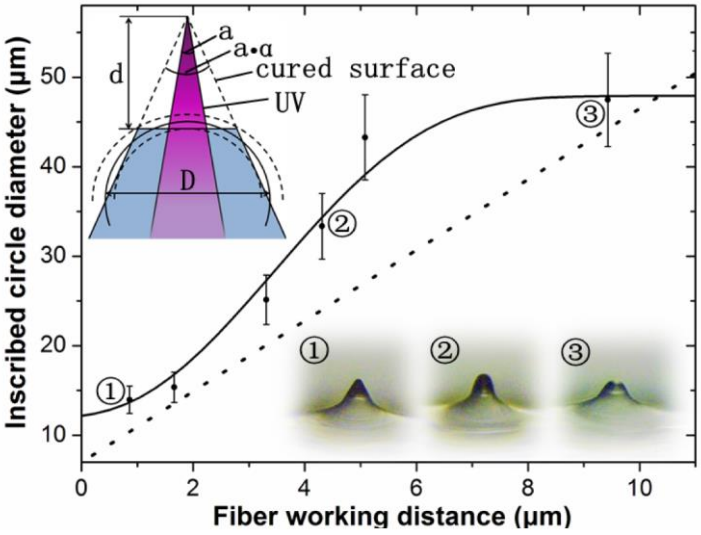

Fig. 4. The sharpness of the fabricated axicons is plotted as a function of the distance between epoxy and fiber-axicon, with dotted line being the calculated result. Inserts (1)-(3) display axicons obtained when fiber working distance (distance between fiber cone tip and upper surface of epoxy) was at 0.95, 3.20, and 9.30μm, respectively.

Furthermore, the sharpness of the fabricated axicon tip was found to be adjustable through changing fiber working distance, i.e., the distance between the fiber-axicon and the UV curable epoxy, as shown in Fig. 4. Here, the sharpness of the axicon lens is quantified as the

#203763 - $15.00 USD Received 3 Jan 2014; revised 21 Mar 2014; accepted 22 Apr 2014; published 1 May 2014

diameter of the smallest inscribed circle in the axicon tip. The sharpest axicon was obtained when the beam waist was exactly located at the upper surface of the epoxy, as shown in Fig. 3 insert (1).

Based on Eq. (1) and (2), we were also able to calculate the theoretical sharpness as a function of working distance. By setting the angle of focused beam according to Fig. 3 and removing the air gap between the fiber tip and upper surface of epoxy, we fit an inscribed circle inside the tip and generated a circle circumscribing the remaining area (as shown in the two dashed circles in the top Fig. 4 insert), then averaged the two diameters to yield an estimated sharpness of fabricated axicon:

$$D = p \cdot d \cdot \frac{\tan(\frac{a\alpha}{2})\left[\tan(\frac{\pi}{4}-\frac{a\alpha}{4})+\sin(\frac{\pi}{4}-\frac{a\alpha}{4})\right]}{\tan(\frac{\pi}{4}-\frac{a\alpha}{4})\sin(\frac{\pi}{4}-\frac{a\alpha}{4})}+c \qquad (3)$$

where p is solidification coefficient at different exposure power, d is the fiber working distance, α the apex angle of the focused beam generated by the fiber axicon, a the coefficient of the change from α to the apex angle of the actual fabricated axicon; c a constant representing zero offset equaling to the smallest diameter of a cured spot that can be made. Using Eq. (3) a dotted curve is plotted in Fig. 4 in comparison with experimental measurement, where α = 42.2°, c = 7μm, and a = 1.33, p = 1.83 as the ratio of fabricated to calculated apex angle depending on (i) fiber cone lens as indicated in Fig. 3 and (ii) laser power and exposure time discussed in next section. Though a thorough model of solidification is much more complicated and would also be a function of the characteristics of photo-sensitizer as well as the individual rings of Bessel beam, Eq. (3) provides a simplified model that estimates the experimental result.

In addition, the size of the axicon can be controlled, proportionally increasing with the thickness of the UV curable epoxy. It was found that this fabrication process can be calibrated and the results are highly reproducible with a precision of better than ± 0.5μm. Subject to the properties of the UV curable epoxy, the illumination intensity and exposure time are determined by the thickness of the epoxy, the geometry of the fabricated axicon, as well as operation temperature. However, the fabrication process was found to be insensitive to exposure time as long as polymerization threshold was reached.

The apex angle of axicons was also studied experimentally in terms of both laser power and exposure time. Considering that height of fabricated axicon varies little due to a given epoxy thickness, it is conceivable that increased laser power is likely to expand the cured region as the power of the beam tail reaches the polymerization threshold of the epoxy, which results in an increase in the apex angle of fabricated axicon (e.g, [19]).

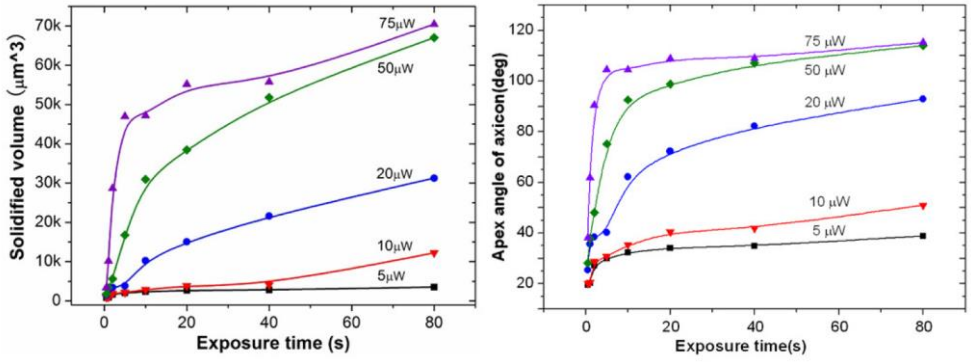

Fig. 5. Solidified volume (left) and apex angle of fabricated axicons (right) as a function of both laser power and exposure time in direct-writing process.

#203763 - $15.00 USD Received 3 Jan 2014; revised 21 Mar 2014; accepted 22 Apr 2014; published 1 May 2014

As shown in Fig. 5, we can evaluate the result through the curves of solidified volume of the fabricated axicons as a function of both exposure time and power influence, and the apex angle of the fabricated axicon is strongly dependent on laser power used in direct-writing process, and is only weakly increased with exposure time. This measurement confirms the postulated formation process of the axicon: the cured region is mostly determined by the area of beam where its intensity is above the polymerization threshold, while accumulation of laser power over time affects very little the apex angle of fabricated axicons. The test used a fiber axicon with an apex angle of 120°, and the layer thickness of the epoxy was set to be 30 μm, with a post-exposure UV treatment of 50 sec.

Finally, by mounting the fiber axicon on a moving two-dimensional translation stage and curing the UV epoxy layer in a sequence, uniformly distributed axicons were formed in a linear array as shown in Fig. 6(A). In a similar process we were able to print an axicon onto the end face of a fiber to achieve a fast replication of the axicon end lens with an apex angle of 37° (apex angle of the fiber-axicon is 110°, laser power 10 μW and exposure time 30 sec), the as displayed in Fig. 6(B).

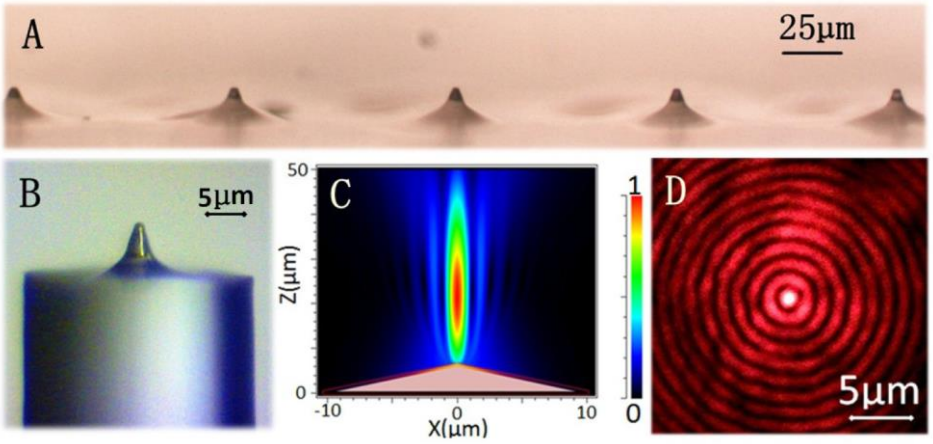

Fig. 6. (A) Microscopic image of a fabricated axicon array. (B) Microscope image of an axicon printed on end surface of a single mode optical fiber. (C) Numerical simulation of the Bessel beam exiting the axicon along the propagation path. (D) Experimental record of a section of the Bessel beam from a fabricated axicon.

An axicon is able to generate a Bessel beam with a smaller FWHM and longer focus length when compared with those of a focused Gaussian beam. Figure 6(C) is a numerical simulation of the generation of the Bessel beam, representing wave propagation of a Gaussian beam with a beam waist of 10 μm through an axicon of 110° cone simulated in software FullWAVE by RSoft Design Group using the finite-difference time-domain (FDTD) method. The calculation is compared to the measured cross-section of the Bessel beam from the fabricated axicon shown in Fig. 6(D), the smallest spot in the propagation path taken 20 μm away from the fabricated axicon. The high intensity in center lobe along with distinguishable ring patterns demonstrates the feasibility of this method to fabricate axicons of a good optical surface finishing.

3. Conclusion

A quasi-Bessel beam was efficiently utilized to form optical 3D structures. It is demonstrated that laser direct writing with a Bessel beam can be used to create 3D optically polymerized micro-axicons with good repeatability and high optical performance. The dimension of the fabricated micro-axicons is in direct proportion to the thickness of UV curable optical epoxy with a precision of ± 0.5μm, and the experimental investigation revealed that the geometrical parameters of resulting axicons can be controlled as functions of laser power, the divergence

#203763 - $15.00 USD Received 3 Jan 2014; revised 21 Mar 2014; accepted 22 Apr 2014; published 1 May 2014

angle of Bessel beam, and the working distance between substrate and focused beam. Theoretical analysis indicated that the geometrical parameters could be estimated using the power distribution of Bessel beam as a function of apex angle. Experimental observation also shows that laser exposure time has a weak effect on the apex angle of fabricated axicons as long as polymerization threshold is reached.

The fabricated axicons have unique focusing performance, and it can be applied in many areas such as optical trapping and optical coupling. This laser direct-writing technique can satisfy the need for a micro-axicon and axicon array fabrication methodology with low-cost, high consistency, and high fabrication rate, and has the potential for practical implementations of 3D polymerization of axicons in photonics, micro-optics and biomedical fields.

Acknowledgments

This work was supported by the National Natural Science Foundation of China (NSFC) under grant 61178049.

#203763 - $15.00 USD Received 3 Jan 2014; revised 21 Mar 2014; accepted 22 Apr 2014; published 1 May 2014